DUAL CANTED UNDULATORS AT THE ADVANCED PHOTON SOURCE*

Patric K. Den Hartog#, Glenn A. Decker, Louis J. Emery
Advanced Photon Source, Argonne National Laboratory, Argonne, IL 60439, USA

Abstract

At the Advanced Photon Source (APS), 34 straight sections are reserved for the installation of insertion devices for users. Each straight section allows space for up to two 2.4-meter-long devices. By sacrificing 0.4 m of undulator from each device and introducing a one milliradian chicane with three small electromagnets, two separate experimental programs can be conducted using the same straight section, thereby potentially doubling the scientific output with the same real estate. The design of the straight section and front end and plans for implementation and commissioning of this scheme at the APS during May 2003 are presented.

INTRODUCTION

The Advanced Photon source is a third-generation synchrotron radiation facility serving a wide variety of users. Since operations began in 1996, 30 of the available sectors have been allocated to various groups. Because of the increasing scarcity of unallocated beam line real estate, new ideas for enhancing productivity from the remaining straight sections have been considered. One of these ideas is the canted undulator (CU) straight section. In this configuration, a chicane is created with a trio of dipole magnets with an undulator in each leg (Figure 1). The result is an angular separation between the x-ray beams that can be exploited downstream to create two independent beam lines from a single straight section. The first application of the CU scheme at APS was implemented for an experimental program in polarization studies that uses both hard (>3 keV) and soft (0.5 – 3 keV) x-rays. A 270 µrad separation between the two x-ray beams was created with permanent magnet dipoles.

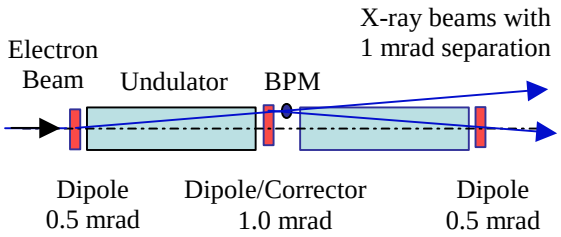

Figure 1. Schematic layout of a CU straight section showing the angular separation of the x-ray beams produced by the three dipoles. The dipoles are placed symmetric about the center of the straight section and the BPM is displaced 113 mm downstream.

Deflecting the soft x-ray beam outward using a pair of horizontally deflecting mirrors further increased the separation between beam lines. This scheme was successfully implemented in 1999 [1]. For programs requiring two hard x-ray beams, however, additional angular separation of the x-ray beams by the dipoles is required as the deflecting mirrors lose their effectiveness at higher energies.

CU BEAM LINES

Protein crystallography experiments have grown in importance at many synchrotron facilities, occupying a growing proportion of the available beam lines. The unparalleled brilliance of third-generation facilities has made high throughput possible but in many cases the maximum usable x-ray flux is determined by sample lifetime. Typically the biology beam lines operate with only a single 2.4-m-long undulator in the 5-m-long straight section. Thus the research programs can benefit if more beam lines can be built within the available experimental floor space. The tradeoff is a somewhat reduced available length for undulators and a concurrent reduction in the x-ray flux and brilliance. Still, for some groups the gain in experiment throughput more than compensates the reduction in x-rays. Three new groups at APS are currently planning to use the CU arrangement.

CU COMPONENTS

The CU system consists of two shortened undulators, a special insertion device vacuum chamber, dipoles, and a corrector for the chicane and a specialized front end.

Undulators

The standard undulator used at the APS is a 2.4-m-long 3.3-cm-period hybrid planar magnetic structure mounted on a welded aluminum strongback [2]. To make room for the chicane dipoles, 5 periods were removed from each end. The strongback is normally supported by a gap-separation mechanism at the Airy points (.22315L from each end) to minimize the distortion of the magnetic structure by equalizing the droop of the overhanging ends and of the sag at the midpoint between the two supports. The reduction in magnetic attraction force at the ends causes an increase in the overall amplitude of the droop. Finite element calculations of the structure suggested that the deformation was within tolerances, which was confirmed by magnetic measurements [3].

ID Vacuum Chamber

APS has designed a number of small-aperture insertion device (ID) vacuum chambers based on aluminum extrusions [4]. Recently, a new extrusion was developed that changed the profile from an ellipse to an oval [5]. This new profile was used for the CU straight section. A

* Supported by the U.S. Dept. of Energy, BES-Materials Sciences, under Contract No. W-31-109-Eng-38.
#PDenHartog@anl.gov

capacitive RF beam position monitor (BPM) was located at the center of the chamber, between the undulators, and displaced outboard horizontally 1.18 mm to match the electron beam trajectory.

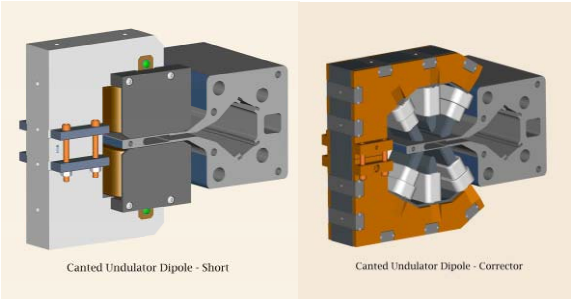

Figure 2. Short dipole (left) and corrector magnet.

Dipoles and Correctors

In order to provide maximum flexibility for operation of the storage ring, electromagnets were chosen for the dipoles. To maintain the symmetry of the chicane, the center dipole was designed to be twice as long as the end dipoles but with the same field. All three magnets are operated in series with a single power supply.

Although the IDs are designed and tuned to eliminate gap-dependent steering, some small residual remains (<30 Gauss-cm first integral and <61,000 Gauss-cm^2 second integral). In order to maintain the independence of the two beam lines, an x-y corrector was installed between the IDs that allows up to 30 µrad of steering correction. In this way, minor steering variations of the first undulator can be compensated with the APS feed-forward beam stabilization system [6] so as to eliminate any effect on the trajectory of the inboard beam by the first undulator. All of the steering magnets, including the x-y corrector, were designed to be installed over an existing ID vacuum chamber (Figure 2). The two undulators, three dipoles, and corrector were measured magnetically as a group on the APS 6 m bench. No gap dependence of the magnetic field was seen due to the proximity of the dipole magnets to the undulator magnetic structure. One possible failure mode occurs if the three dipole magnets responsible for the 1-mrad separation are de-energized, resulting in two co-linear x-ray beams, exceeding the front-end thermal design limits. For this reason, the power supply will be interlocked to the machine protection system and the stored beam will be dumped when $I_{mag} < 0.75\ I_{nominal}$ and $I_{SR} > 130$ mA.

Front End

A major challenge of the CU design was the thermal load on the front end [7]. The original front ends installed at the APS were designed to allow operation with a maximum x-ray power of 6.6 kW and maximum normal incidence power density of 0.6 kW/mm^2 [8]. Later versions of the front end were designed for 9 kW total power and 0.8 kW/mm^2 power density. Because of the desire to increase the stored beam current at APS in the future, it was decided to design for a maximum allowable stored beam of 200 mA. This placed a severe constraint on the design of the first mask and first photon shutter. Also, the horizontal displacement of the two beams required that the glancing incidence surface of the photon shutters be horizontal rather than vertical, which would have been desirable from the standpoint of reducing the incident power density. Shu et al. [8] developed a V-shaped shutter for the previous front end version 1.5 that could withstand 12 kW of total power, but this design was not practical for two separated beams. The requirement to absorb two separate x-ray beams led to a unique design for the photon shutters. The chosen design intercepts the beams on a horizontal Glidcop® strike plate in the closed position and functions as a vertical mask in the open position. Glidcop plate, chosen for its superior strength

Table 1: Canted Undulator Front End Parameters

Stored beam current (mA)	200	
Total power from two undulators (kW)	20.4	
Power density at normal incidence (kW/mrad^2)	281	
Temperature and equivalent stress for h=0.015 W/mm^2°C, T_0=20 °C)	**PS1**	**PS2**
Incident angle	0.91°	0.91°
Peak normal incidence power density (kW/mm^2)	0.79	0.64
Peak incident power density (W/mm^2)	12.7	10.4
T_{max} on Glidcop® strike surface (°C)	278	248
T_{max} on OFHC copper (°C)	180	163
T_{wall} of cooling channel (°C)	143	129
Maximum stress, σ_{eff} (MPa)	394	347
Temperature and equivalent stress for h=0.015 W/mm^2°C, T_0=20 °C)	**FM1**	**FM2**
Distance from center of straight section (m)	16.9	17.7
Inlet aperture (mm)	[64 x 26]	[46 x 17]
Exit aperture (mm)	[40 x 14]	[26 x 5]
Device active length (mm)	600	600
Vertical taper angle	0.57°	0.57°
Horizontal taper angle	1.15°	0.95°
Peak normal incidence power density (kW/mm^2)	1.10	1.02
Peak vertical incidence power density (W/mm^2)	11.0	10.1
Peak horizontal incidence power density (W/mm^2)	22.2	16.8
T_{max} on Glidcop® strike surface (°C)	218	198
Maximum stress, σ_{eff} (MPa)	397	333

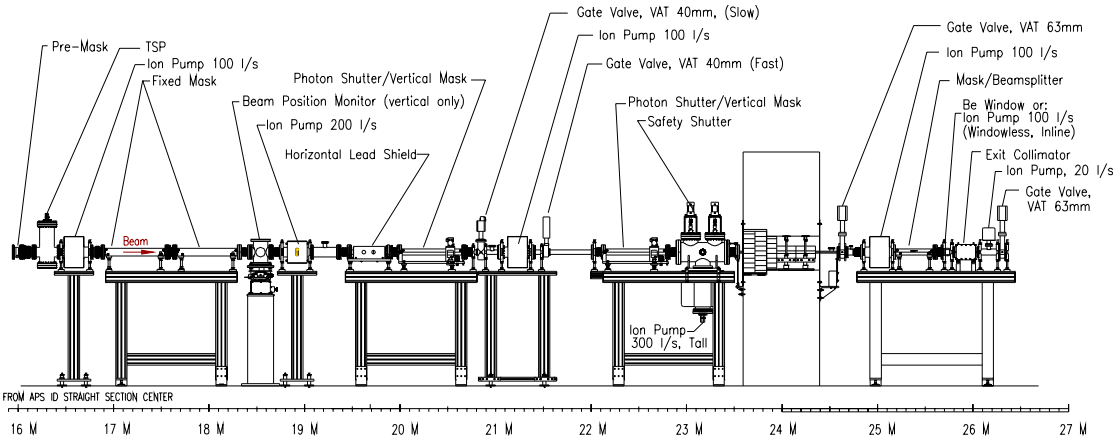

Figure 4. Layout of the components of the front end for the canted undulator beam lines.

compared to Glidcop bars or rounds, was brazed to the top internal surface of the Cu body. The lower OFHC Cu surface can only see a missteered beam in the open position at highly glancing angle (0.24°). The relatively small separation of the beams at the entrance of the front end also contributed to a difficult thermal engineering challenge. To enhance the film coefficient, h, all of the high-heat-load components have spring inserts in the cooling channels [9]. These inserts are much less prone to corrosion or erosion than the wire mesh that was used in earlier front-end components. Also, since the pressure drop due to the wire coils is much less than with the wire mesh, the saturation temperature rises. With a typical inlet pressure of 110 psig, the output pressure is > 75 psig and the minimum saturation temperature is 160°. Table 1 shows the thermal design limits for the system, the two photon shutters, PS1 and PS2, and the two fixed masks, FM1 and FM2. Design rules of T_{max} < 300° C and σ_{eff} < 450 MPa were used in order to limit the risk of fatigue failure due to thermal cycling. Figure 4 shows a layout of the front end for a CU beam line.

BEAM MISSTEERING LIMITS

The storage ring components are protected from an errant photon beam by a beam position limit detection (BPLD) system. When the 1-mrad dipoles are correctly powered, the two x-ray beams will move together under the influence of accidental closed orbit perturbations. For this reason, beam position monitors mounted on the extreme ends of the insertion device vacuum chamber trigger the machine protection system if the average trajectory through the two devices exceeds predefined limits, i.e., the beam is dumped within 500 microseconds when one of the BPMs at the ends of the straight section exceeds pre-calculated limits. The system is armed when one of the ID gaps is closed below 60 mm. For normal straight sections, the BPLD horizontal limits are calculated for an angle missteering of ± 0.9 mrad. For the CU, the limit will be 0.4 mrad, which is a significant reduction. For optimized steering through the front end, we are aligning the beam line and the accelerator components in a consistent way and expect the beam to be well centered in the rf BPMs and the probability of false trips to be very low.

REFERENCES

[1] J. W. Freeland, J. C. Lang, G. Srajer et al., Rev. Sci. Instrum. **73** (3), 1408 (2002).

[2] E. R. Moog, I. Vasserman, M. Borland et al., in *Proc. 1997 Particle Accelerator Conference*, edited by M. Comyn, M.K. Craddock, M. Reiser et al. (IEEE, 1997), pp. 3224.

[3] M. Erdmann, B. Brajuskovic, and P. Den Hartog, in *Proc. of the 2003 Sync. Rad. Instrm. Conf. (to be published)*.

[4] P. Den Hartog, J. Gagliano, G. Goeppner et al., in *Proc. 2001 Particle Accelerator Conf.* (IEEE, 2001), pp. 607.

[5] E. Trakhtenberg, G. Wiemerslage, and P. Den Hartog, in *these proceedings* (2003).

[6] G. Decker and O. Singh, in *Proc. of the 8th Internat'l. Conf. on Accelerators and Large Experimental Physics Control Systems* (SLAC, 2002), pp. 249.

[7] Y. Jaski, E. Trakhtenberg, J. Collins et al., in *Proc. of the 2nd International Workshop on Mechanical Engineering Design of Synchrotron Radiation Equipment and Instrumentation*, edited by S. Sharma (ANL, Argonne, IL, 2003), pp. 390.

[8] D. Shu, M. Ramanathan, and T. M. Kuzay, Nucl. Instrum. Methods **A 467-468** (1), 762 (2001).

[9] J. Collins, C Conley, and J. Attig, in *Proc. of the 2nd International Workshop on Mechanical Engineering Design of Synchrotron Radiation Equipment and Instrumentation*, edited by S. Sharma (ANL, Argonne, IL, 2003), pp. 409.